Anal. Chem. **2006,** *78,* 484−492

Instrumentation for Multidimensional Luminescence Spectroscopy and Its Application to Low-Temperature Analysis in Shpol'skii Matrixes and Optically Scattering Media

Andres D. Campiglia,* Adam J. Bystol, and Shenjiang Yu

Department of Chemistry, P.O. Box 25000, University of Central Florida, Orlando, Florida 32816-2366

We present a single instrument with the capability to collect multidimensional data formats in both the fluorescence and the phosphorescence time domains. We also demonstrate the ability to perform luminescence measurements in highly scattering media by comparing the precision of measurements in Shpol'skii solvents to those obtained in "snowlike" matrixes and solid samples. For decades, conventional low-temperature methodology has been restricted to optically transparent media. This restriction has limited its application to organic solvents that freeze into a glass. We remove this limitation with the use of cryogenic fiber-optic probes.

The multidimensional nature of photoluminescence provides fluorescence and phosphorescence techniques with unique potential for the direct analysis of target compounds in complex matrixes. The combination of excitation and emission spectra to lifetime information within the fluorescence or phosphorescence time domain gives at least three qualitative parameters for compound determination, namely, one excitation and emission wavelength and one lifetime. The simplicity of the experimental procedure makes room-temperature fluorescence the most popular approach. Fluorescence is readily observed from liquid solutions with no need for sample deoxygenation. Room-temperature phosphorescence is rarely observed from liquid solutions but it can be enhanced with the use of solid substrates,[1−4] micelle-stabilized aqueous solutions,[5−7] or heavy-atom salts.[8,9] In all three phosphorescence approaches, sample deoxygenation is crucial to avoid quenching of the triplet excited state.

The main limitation of room-temperature fluorescence and phosphorescence techniques toward the selectivity of analysis is the broad nature of excitation and luminescence (fluorescence and phosphorescence) spectra. Similar to room-temperature absorption techniques, the diffuse character of such spectra limits their information content and drastically reduces the selective potential for the analysis of target compounds in complex matrixes. Several strategies exist to improve the specificity of luminescence techniques, including reducing the sample temperature to enhance vibronic spectral resolution,[10,11] collection of multidimensional data formats,[12,13] and time-resolved spectroscopy (lifetime measurements).[14−16]

Reducing the sample temperature offers several advantages. Luminescence quantum yields often increase, and the complications of oxygen quenching and energy transfer are eliminated. But the temperature effects on luminescence are specially pronounced in the so-called high-resolution techniques, namely, Shpol'skii spectroscopy (SS) and fluorescence line narrowing spectroscopy. In these techniques, the sharp spectra with vibrational information result from homogeneous and inhomogeneous band-broadening reduction.[17−20]

Research in our group has focused on exploring the full potential of SS with a significant selectivity enhancement based on information-rich multidimensional data formats. We have shown that the combination of a pulsed tunable dye laser, a pulsed delay generator, a spectrograph, and an intensifier-charged

* To whom correspondence should be addressed. E-mail: acampigl@mail.ucf.edu.

(1) Escandar, G. M. *Appl. Spectrosc.* **2004**, *58*, 836−842.
(2) Traviesa-Alvarez, J. M.; Costa-Fernandez, J. M.; Pereiro, R.; Sanz-Medel, A. *Talanta* **2004**, *62*, 827−833.
(3) Arruda, A. F.; Goicoechea, H. C.; Santos, M.; Campiglia, A. D.; Olivieri, A. C. *Environ. Sci. Technol.* **2003**, *37*, 1385−1391.
(4) Mendonsa, S. D.; Hurtubise, R. J. *J. Luminesc.* **2002**, *97*, 19−33.
(5) Kuijt, J.; Ariese, F.; Brinkman, U. A. T.; Gooijer, C. *Anal. Chim. Acta* **2003**, *488*, 135−171.
(6) Arancibia, J. A.; Escandar, G. M. *Analyst* **2001**, *126*, 917−922.
(7) Diaz, B. C.; Terrones, S. C.; Carretero A. S.; Fernandez, J. M. C.; Gutierrez, A. F. *Anal. BioAnal. Chem.* **2004**, *379*, 30−34.
(8) Thompson, A. L.; Hurtubise, R. J. *Appl. Spectrosc.* **2005**, *59*, 126−133.
(9) Castillo, A. S.; Carretero, A. S.; Fernandez, J. M. C.; Jin, W. J.; Gutierrez, A. F. *Anal. Chim. Acta* **2004**, *516*, 213−220.
(10) Hurtubise, R. J. *Phosphorimetry: Theory, Instrumentation and Applications*; VCH: New York, 1990.
(11) Vo-Dinh, Fetzer, J., Campiglia, A. D. *Talanta* **1998**, *47*, 943−969.
(12) Ho, C., −N.; Warner, I. M. *Anal. Chem.* **1982**, *54*, 2486−2491.
(13) Warner, I. M.; Patonay, G.; Thomas, M. P. *Anal. Chem.* **1985**, *57*, 463A−483A.
(14) Knorr, F. J.; Harris, J. M. *Anal. Chem.* **1981**, *53*, 272−276.
(15) McGown, L. B. *Anal. Chem.* **1989**, *61*, 839A−847A.
(16) Smalley, M. B.; Shaver, J. M.; McGown, L. B. *Anal. Chem.* **1993**, *65*, 3466−3472.
(17) Gooijer, C.; Ariese, F.; Hofstraat, J. W. Shpol'skii Spectroscopy and Other Site-Selection Methods: Applications in Environmental Analysis, Bioanalytical Chemistry, and Chemical Physics. In *Chemical Analysis: A Series of Monographs on Analytical Chemistry and Its Applications*; Winefordner, J. D., Ed.; Wiley-Interscience: New York, 2000; Vol. 156.
(18) Luthe, G.; Es−Sbai, H.; Gooijer, C.; Brinkman, U. A. T.; Ariese, F. *Anal. Chim. Acta* **2002**, *459*, 53−59.
(19) Kozin, I.; Gooijer, C.; Velthorst, N. H.; Hellou, J.; Zitko, V. *Chemosphere* **1996**, *33*, 1435−1477.
(20) Gooijer, C.; Ariese, F.; Hofstraat, J. W.; Velthorst, N. H. *Trends Anal. Chem.* **1994**, *13*, 53−61.

10.1021/ac051332v CCC: $33.50
Published on Web 12/07/2005

coupled device (ICCD) is well suited for the rapid collection of wavelength−time matrixes (WTMs), excitation−emission matrixes (EEMs), and time-resolved excitation emission matrixes (TREEMs) in the fluorescence time domain (ns to μs).[21,22] Adding the temporal dimension to the highly resolved Shpol'skii spectra provides

an extremely selective tool for the determination of structural isomers in complex matrixes with numerous PAHs. Unambiguous isomer identification is made possible on the bases of spectral and lifetime analysis. Fluorescence decays report on spectral peak purity, an important parameter for accurate quantitative analysis.[23−26]

Another significant improvement is the introduction of cryogenic fiber-optic probes for sample freezing at 77 and 4.2 K. It is possible now to routinely perform measurements at liquid nitrogen and helium temperatures; frozen samples are prepared in a matter of seconds. During the course of our experiments, we noticed the significant contribution of phosphorescence to the steady-state emission spectra of numerous PAHs, polychlorinated biphenyls, polychlorinated dibenzofurans, and polychlorinated dioxins imbedded in Shpol'skii matrixes. New instrumentation was then developed to handle the relatively long phosphorescence lifetimes (ms−s) at 77 and 4.2 K.[27,28] The rather large lifetime differences observed from compounds within the same polycyclic aromatic class and the excellent analytical figures of merit provided a solid foundation for including phosphorescence data formats in the multidimensional analyses in complex samples.

In this article, we present a single instrument with the capability to collect multidimensional data formats in both the fluorescence and the phosphorescence time domains. We also demonstrate the ability to perform luminescence measurements in highly scattering media by comparing the precision of measurements in Shpol'skii solvents to those obtained in "snowlike" matrixes and solid samples. For decades, conventional low-temperature methodology has been restricted to optically transparent media. This restriction has limited its application to organic solvents that freeze into a glass. In this article, we remove this limitation with the use of cryogenic fiber-optic probes.

EXPERIMENTAL SECTION

Chemicals and Solution Preparation. All chemicals were analytical reagent grade and used without further purification. Otherwise noted, Nanopure water was used throughout. PAHs were purchased from Aldrich at their highest available purity. HPLC grade solvents (Sigma-Aldrich) were used to prepare stock PAH solutions. Working solutions were prepared by diluting the stock solution with the appropriate solvent (HPLC grade) prior to luminescence measurements. Rhodamine 6G, DCM, LDS 698, and LDS 759 were purchased from Exciton and used with the tunable dye laser according to specifications. Their tuning ranges were 275−290, 300−340, 330−370, and 350−395 nm, respectively. Dye exchange was made easy with the use of one pump per laser dye.

Survey of Excitation and Emission Spectra at Room Temperature and 77 K. The 77 K excitation and emission spectra were acquired with a commercial spectrofluorometer (Photon Technology International). For fluorescence measurements, the excitation source was a continuous wave 75-W xenon lamp with broadband illumination from 200 to 2000 nm. Detection was made with a photomultiplier tube (PMT, model 1527) with spectral response from 185 to 650 nm. For phosphorescence measurements, the excitation source was a pulsed 75-W xenon lamp (wavelength range from 200 to 2000 nm) with variable repetition rate from 0 to 100 pulses/s and a pulse width of ~3 μs. Detection was made by means of a gated analog PMT (model R928) with extended wavelength range from 185 to 900 nm. The excitation and emission monochromators had the same reciprocal linear dispersion (4 nm·mm^{-1}) and accuracy (±1 nm with 0.25-nm resolution). Their 1200 grooves/mm gratings were blazed at 300 and 400 nm, respectively. Wavelength reproducibility was ~±2 nm. The instrument was computer controlled using commercial software (Felix32) specifically designed for the system. Correction of emission and excitation spectra was made in postacquisition mode to compensate for wavelength dependence of detector sensitivity and excitation light source, respectively.

Cryogenic Fiber-Optic Probe (FOP). The FOP consisted of one delivery and six collection fibers. All the fibers were 3-m-long and 500-μm-core diameter silica-clad silica with polyimide buffer coating (Polymicro Technologies, Inc.). The fibers were fed into a 1.2-m-long section of copper tubing that provided mechanical support for lowering the probe into the liquid helium. At the sample end, the fibers were arranged in a conventional six-around-one configuration with the delivery fiber in the center, bundled with vacuum epoxy (Torr-Seal, Varian Vacuum Products), and fed into a metal sleeve for mechanical support. The copper tubing was flared stopping a Swage nut tapped to allow for the threading of a 0.75-mL polypropylene sample vial. At the measurement end, the collection fibers were bundled with vacuum epoxy into a slit configuration, fed into a metal sleeve, and aligned with the entrance slit of the spectrometer.

Instrumentation for Multidimensional Shpol'skii Spectroscopy. The instrumentation for multidimensional luminescence spectroscopy (MLS) is shown in Figure 1. The major difference to the fluorescence system previously reported[22] is the integration of a mechanical shutter to facilitate phosphorescence spectra and lifetime acquisition. The mechanical shutter (Oriel) is positioned in the path of the dye laser excitation beam prior to launch into the FOP. The shutter has a rise time (open time) of 1.5 ms and fall time (close time) of 3.0 ms with a maximum pulse width of 6.5 ms. The shutter is controlled either manually (always open or always closed) via a switch on the controller front panel or programmatically through a transistor-transient logic (TTL) pulse. This TTL pulse is programmed through the A + B outputs of the digital delay generator (model DG535, Stanford Research Systems,

(21) Bystol, A. J.; Campiglia, A. D.; Gillispie, G. D. *Appl. Spectrosc.* **2000**, *54*, 910−917.
(22) Bystol, A. J.; Campiglia, A. D.; Gillispie, G. D. *Anal. Chem.* **2001**, *73*, 5762−5770.
(23) Bystol, A. J.; Whitcomb, J. L.; Campiglia, A. D. *Environ. Sci. Technol.* **2001**, *35*, 2566−2571.
(24) Bystol, A. J.; Thorstenson, T.; Campiglia, A. D. *Environ. Sci. Technol.* **2002**, *36*, 4424−4429.
(25) Yu, S.; Campiglia, A. D. *Anal. Chem.* **2005**, *77*, 1440−1447.
(26) Goicoechea, H. C.; Yu, S.; Olivieri, A. C.; Campiglia, A. D. *Anal. Chem.* **2005**, *77*, 2608−2616.
(27) Martin, T. L.; Campiglia, A. D. *Appl. Spectrosc.* **2001**, *55*, 1266−1272.
(28) Martin, T. L.; Arruda, A. F.; Campiglia, A. D. *Appl. Spectrosc.* **2002**, *56*, 1354−1360.

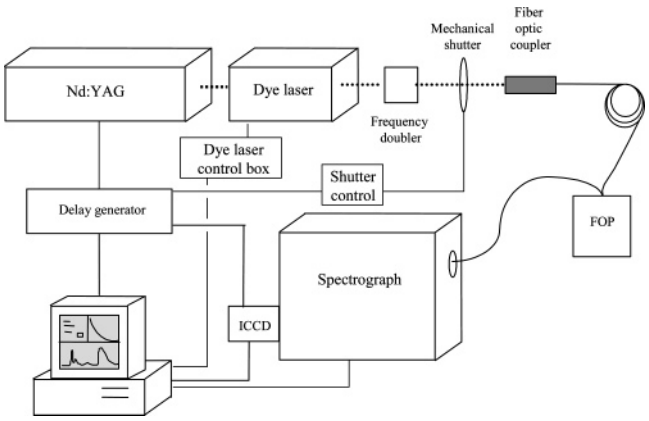

Figure 1. Instrumentation for multidimensional luminescence spectroscopy. FOP, fiber optic probe. ICCD, intensified charge coupled device.

Inc.) via a general purpose interface bus interface from National Instruments.

Excitation energy is generated by directing the output of a Northern Lights tunable dye laser (Dakota Technologies, Inc.) through a KDP frequency-doubling crystal. When pumped with ~30 mJ from the second harmonic generator of a Nd:YAG Q-switched laser (Quanta Ray), it produces more than 5 mJ at peak of Rhodamine 6G in a spectral bandwidth less than 0.03 nm. The multichannel detector consists of a front illuminated ICCD (Andor Technology). The CCD has the following specifications: active area 690 × 256 pixels (26 μm^2 pixel size at photocathode), dark current 0.002 electrons pixel^{-1} s^{-1}, and readout noise 4 electrons at 20 kHz. The ICCD is mounted at the exit focal plane of a spectrograph (SPEX 270M) equipped with a 1200 grooves/mm grating blazed at 500 nm. The distance between the collection probe and the entrance slit of the spectrograph is optimized to completely illuminate the diffraction grating area. The system is operated in the external trigger mode. A trigger signal from the Nd:YAG laser prepulse trigger is sent to the delay generator 140 ns before the laser fires to account for inherent delays in the electrical cables and components.

Collection of Fluorescence Spectra with the MLS. Fluorescence measurements are made on the nanosecond time scale with the mechanical shutter in the open position. Time resolution is achieved with the intensifier in front of the ICCD, which acts as a superfast shutter with a minimum gate of 2 ns (full width at half-maximum). Once triggered by the laser, the pulse delay generator uses this information to determine when the image intensifier in the detector head is gated on (gate delay, D) and for how long it is gated on (gate width, G). These parameters are entered on the control computer with Andor software. The ICCD acquires data while the intensifier is gated on. While the intensifier is gated off, the acquired data are transferred from the detector head to the controller card (32-bit Intelligent Bus-Mastering PCI card) in the computer. Otherwise noted, fluorescence spectra result from the accumulation of emission of 100 laser pulses. This process takes ~10 ms/40-nm spectrum. If a wavelength range larger than 40 nm is of interest, the spectrograph is tuned to the new wavelength range and the process is repeated.

Collection of Phosphorescence Spectra with the MLS. Depending on the strength and the duration of the phosphorescence emission, spectra are collected by one of two procedures. For PAHs that generate enough phosphorescence photons per laser pulse and have relatively short lifetimes (less than 40 ms), the use of the mechanical shutter is not necessary. The sequence of events is the same as the one used for collecting fluorescence spectra, but the delay and gate times are set at a much longer time scale. Typical delay and gate times were 20 μs and 40 ms, respectively. The delay was long enough to eliminate sample and background fluorescence, and the gate time was the maximum gate allowed for each firing of the laser. Our YAG laser fired every 100 ms (10 Hz), and because ~50 ms was needed between shots for DTS, gate times longer than 40 ms would result in convolution of the collected data with the next laser shot. The use of a faster computer could certainly decrease DTS time.

The mechanical shutter comes on handy for PAHs that exhibit weak phosphorescence intensity and relatively long phosphorescence lifetimes. The pulse delay generator controls the timing for both the shutter and the intensifier on the ICCD. During the excitation cycle, the pulse generator is triggered by the laser to set the shutter to the open position for a certain number of pulses (typically 20 pulses). During the emission cycle, the shutter is closed and the phosphorescence decay is recorded. The closing of the shutter sets the "zero reference time" for the delay time and the gate time on the ICCD. This method allows one to build up the triplet-state population to an acceptable signal-to-noise ratio. It also allows for gate times in excess of 40 ms to be used without concern of overlapping laser pulses.

Collection of Fluorescence and Phosphorescence WTMs. Figure 2A depicts the series of events leading to fluorescence WTM collection. The duration of the steps by which the gate delay is progressively increased in the course of the sequence of acquisitions (gate step = $D_I - D_{I-1}$, where $I = 2, ..., N$) is entered on the control computer with Andor software. For collecting phosphorescence WTMs from PAHs with strong phosphorescence and relatively short phosphorescence lifetimes (less than 40 ms), the sequence of events is the same but D and G are set at much longer time scales (ms). Figure 2B shows the sequence of events for collecting WTMs from PAHs with weak phosphorescence and relatively long phosphorescence lifetimes (longer than 40 ms). Instead of using the laser pulse as the "zero reference time", the series of phosphorescence spectra is taken at incremental delay times from the closing of the shutter. For relatively long phosphorescence lifetimes, this method results in very long acquisition times, typically 1 h or more per WTM. The alternative method is depicted in Figure 2C. It involves exciting the PAH for several seconds to build up the triplet-state population, closing the shutter, and then collecting the time-resolve emission over several seconds. The resulting WTM consists of many spectra with a delay step equal to the firing rate of the laser (100 ms). Since each spectrum is an accumulation of only one laser shot, many WTMs (typically 100) need to be accumulated to average out the effects of noise. This averaging is, in effect, similar to accumulating 100 laser shots at each delay increment, as in fluorescence WTM collection. Because the delay is eliminated from each acquisition cycle, the time it takes to collect a full WTM is considerably reduced. Collecting 100 WTMs over a total period of 5 s each takes ~9 min.

Fluorescence and Phosphorescence Lifetimes with the MLS. Fluorescence and phosphorescence lifetimes were obtained

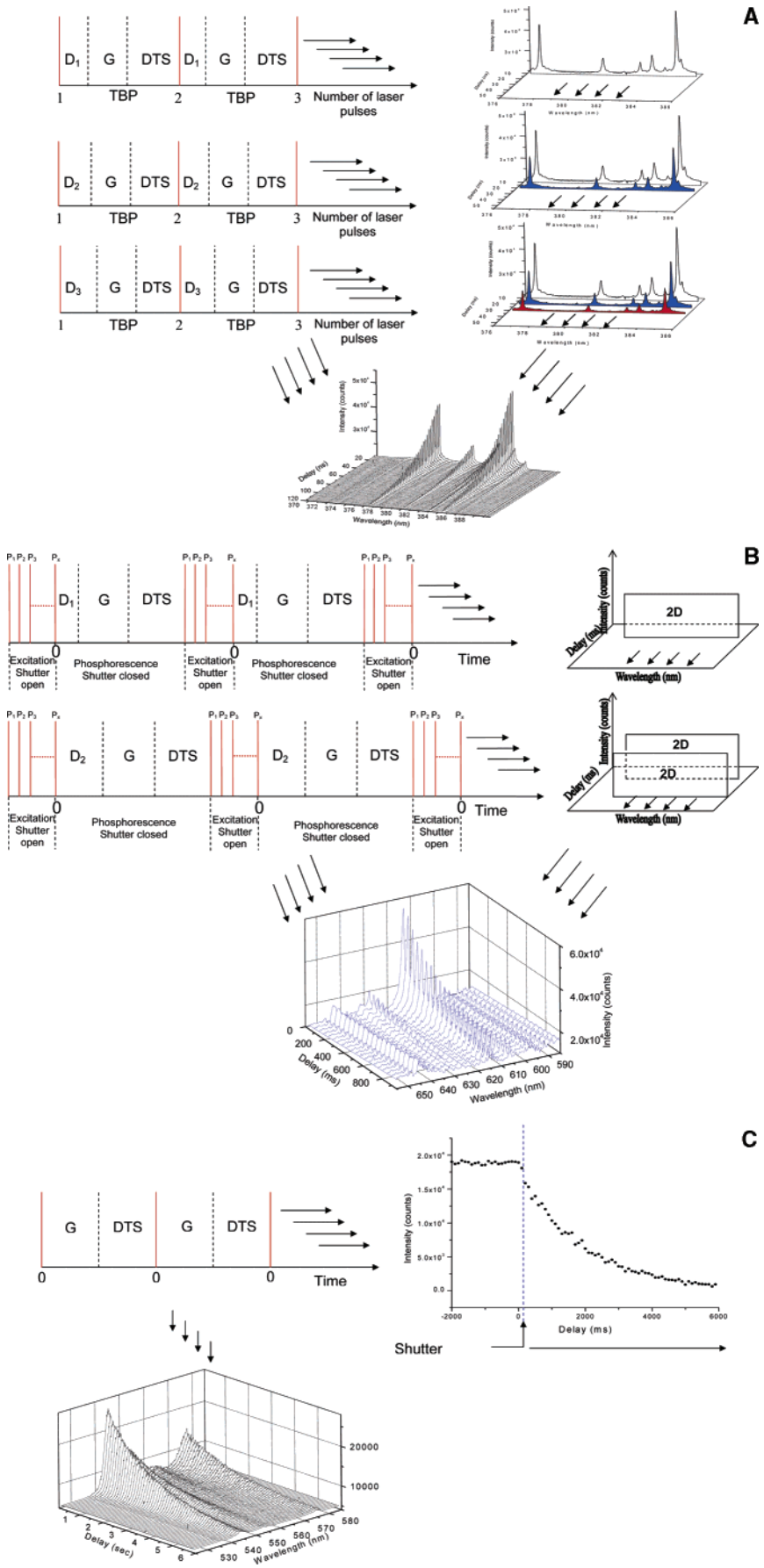

Figure 2. Sequence of events leading to WTM collection of (A) fluorescence, (B) weak phosphorescence and lifetimes shorter than 40 ms, and (C) weak phosphorescence and lifetimes longer than 40 ms. P, laser pulse; D, delay time; G, gate time; DTS, data transfer and storage; TBP, time between pulses.

via a three-step procedure: (1) full sample and background WTM collection; (2) Background decay curve subtraction from the fluorescence or phosphorescence decay curve at a wavelength of maximum emission for each PAH; and (3) fitting of the background-corrected data to single-exponential decays. Origin software (version 5, Micronal Software, Inc.) was used for curve fitting of fluorescence and phosphorescence lifetimes. Fitted decay curves ($y = y_0 + A_1 \exp^{-(x-x_0)t_1}$) were obtained by fixing x_0 and y_0 at a value of zero.

Software for Phosphorescence Measurements. The Andor software was unable to handle the very long delay and gate times required for data acquisition. We were able to collect individual spectra with relatively long delay and gate times, but the software failed when we attempted to collect phosphorescence WTM. We circumvented these problems by authoring custom acquisition software with LabView (National Instruments, version 6.0).

Sample Procedures. *77 K Measurements of Liquid Solutions with the Spectrofluorometer.* Measurements followed the classic procedure of immersing the sample solution in a quartz tube into a nitrogen-filled Dewar flask.

77 and 4.2 K Measurements of Liquid Solutions with the FOP. After a known volume of solution was pipetted into the sample vial (typically 100 μL), the tip of the probe was positioned and held constant with the screw cap below the solution surface. The dimensions of the vial were as follows: 30-mm length, 5.5-mm inner diameter, and 7-mm outer diameter. Its maximum volume capacity was 750 μL. Sample freezing was accomplished by lowering the copper tubing into the liquid cryogen. The liquid nitrogen and liquid helium were held in two separate Dewars with 5- and 60-L storage capacity, respectively. The 60-L liquid helium typically lasts three weeks of daily use, averaging 15−20 samples/day. At both temperatures, complete sample freezing takes less than 90 s.

The ~1-min probe cleanup procedure involved removing the sample vial from the cryogen container, melting the frozen matrix, and warming the resulting solution to approximately room temperature with a heat gun, rinsing the probe with *n*-alkane, and drying it with warm air from the heat gun. The entire freeze, thaw, and cleanup cycle took no longer than 5 min.

77 and 4.2 K Measurements from Extraction Membranes with the FOP. The 47-mm solid−liquid extraction membranes were dissected into several 5.6-mm disks using a no. 3 cork borer. A 5.6-mm membrane was placed into the stainless steel filter syringe kit (Alltech) and attached to a 10-mL syringe (Hamilton). PAH extraction from aqueous samples was carried out following a previously described procedure that guarantees ~100% extraction efficiency.[23,24] The membrane was first conditioned with 1 mL of methanol followed by 5 mL of Nanopure water. A 10-mL volume of sample solution (80/20 water/methanol v/v) was passed through the disk to a flow rate of ~30 mL·min^{-1}. Void water was removed from the membrane by forcing three 100-mL volumes of air through the disk using a 100-mL syringe. The membrane was then placed on the bottom of the FOP sample vial with the extracting side facing up, followed by attachment of the probe. The fiber-optic bundle was arranged vertically to ~1 cm above the membrane. This distance provided excitation of the entire disk surface. The FOP was then immersed in the liquid cryogen as previously described. Because there was no physical contact between the fiber and the membrane, fiber cleanup between samples was not necessary.

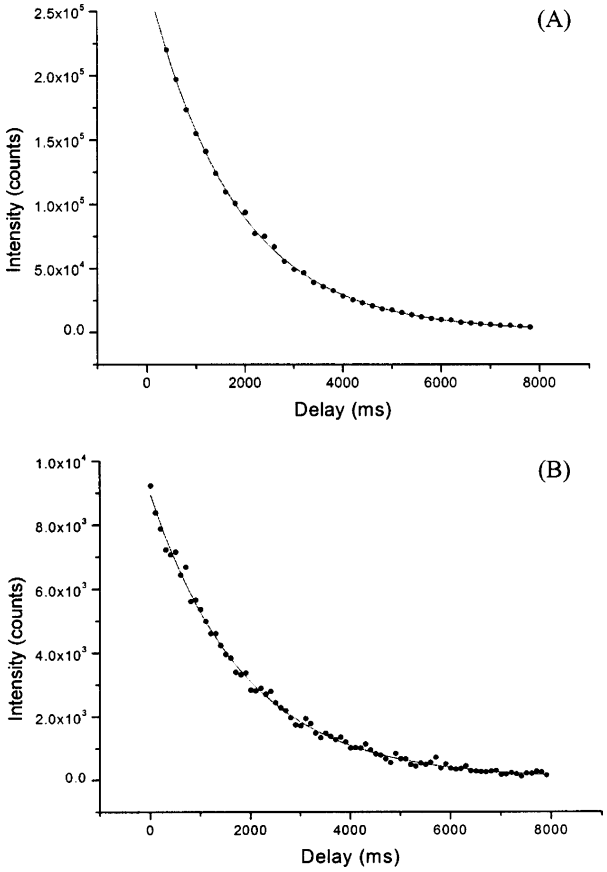

Figure 3. Fitted phosphorescence decay curves for 0.2 μg/mL benzo[*e*]pyrene in *n*-octane at 4.2 K. (A) Fitted decay using data acquisition mode shown in Figure 2B. Gate step of 200 ms and gate width of 2000 ms. (B) Fitted decay using real-time data acquisition mode with gate width of 40 ms and gate step of 100 ms.

RESULTS AND DISCUSSION

Phosphorescence WTM and Lifetime Analysis in Shpol'skii Matrixes. The accuracy and precision of fluorescence WTM collection and fluorescence lifetime analysis in Shpol'skii matrixes have been previously demonstrated.[21,22] Here, we concentrate our efforts on discussing phosphorescence lifetimes and phosphorescence WTM collection with the MLS. The accuracy and precision of measurements was investigated with phosphorescent PAHs previously studied in our laboratory.[27−29] The data obtained with the MLS were then compared to data obtained with the dedicated phosphorescence system.[28]

Phosphorescence WTM can be collected in either the same manner as fluorescence WTM or in a "real-time" fashion. Figure 3 shows the fitted decay curves obtained for benzo[*e*]pyrene in *n*-octane at 4.2 K using the sequence of events shown in Figure 2B and C. Benzo[*e*]pyrene in *n*-octane is a well-known example of a single-site Shpol'skii system.[17,30] The decay in Figure 3A was stripped from a WTM consisting of 100 accumulations with a delay incremented of 200 ms and a gate time of 1000 ms. In Figure 2C

(29) Arruda, A. F.; Yu, S.; Campiglia, A. D. *Talanta* **2003**, *59*, 1199−1211.
(30) Miller, J. C.; Miller, J. N. *Statistics for Analytical Chemistry*; Wiley: New York, 1984.

Table 1. Comparison of Benzo[*e*]pyrene Phosphorescence Lifetimes Obtained with Dedicated Phosphorescence Instrumentation (DPI) and the Multidimensional Luminescence System[a]

instrument/method[b]	4.2 K (ms)[c]
DPI	1787 ± 39 (2.20)
MLS-normal mode	1777 ± 31 (1.74)
MLS-real time mode	1780 ± 60 (3.37)

[a] Excitation and emission wavelengths for all measurements were 386.8 and 614.6 nm, respectively. Benzo[*e*]pyrene concentration was 0.2 $\mu g \cdot mL^{-1}$. [b] Normal mode: many two-dimensional spectra (100 laser shots) collected at incremental delay times. Real-time mode: 100 WTM collected and averaged where each two-dimensional spectrum represents emission resulting from 1 laser shot. [c] Average phosphorescence lifetime of six separate frozen aliquots. Values in parentheses represent the relative standard deviation (%) of six measurements.

Table 2. Fluorescence and Phosphorescence Lifetimes[a] at Different Sites of Chrysene in *n*-Octane at 4.2 K Recorded with the MLS

	fluorescence		phosphorescence	
site	λ (nm)	τ (ns)	λ (nm)	τ (ms)
1	359.2	58.3 ± 1.5	499.1	2078 ± 63
2	359.6	63.4 ± 2.1	500.3	2369 ± 83
3	360.0	60.4 ± 0.8	500.8	2154 ± 56

[a] Fluorescence and phosphorescence lifetimes resulting from measurement of six separate sample aliquots of a 0.2 $\mu g \cdot mL^{-1}$ solution. Excitation wavelength, 321.4 nm.

("real-time mode"), the delay increment of the WTM was equal to the laser duty cycle (100 ms) with a gate of 40 ms. Both decays fitted single-exponential decays with no significant trends in the residuals of the fit. Table 1 compares these lifetimes to those measured with dedicated phosphorescence instrumentation. Within 95% of confidence level ($\alpha = 0.05$), the lifetime averages from individual measurements of six frozen samples were statistically equivalent ($N_1 = N_2 = N_3 = 6$),[30] demonstrating the ability of the new instrument to collect accurate phosphorescence lifetimes. The relative standard deviations were lower than 3.4%, showing excellent precision of measurements as well.

Table 2 summaries the 4.2 K fluorescence and phosphorescence lifetimes of a multisite Shpol'skii system. Chrysene in *n*-octane exhibits emission spectra with three major 0−0 peaks appearing at 359.2, 359.6, and 360.6 nm for fluorescence and 499.1, 500.3, and 500.8 nm for phosphorescence. As we previously

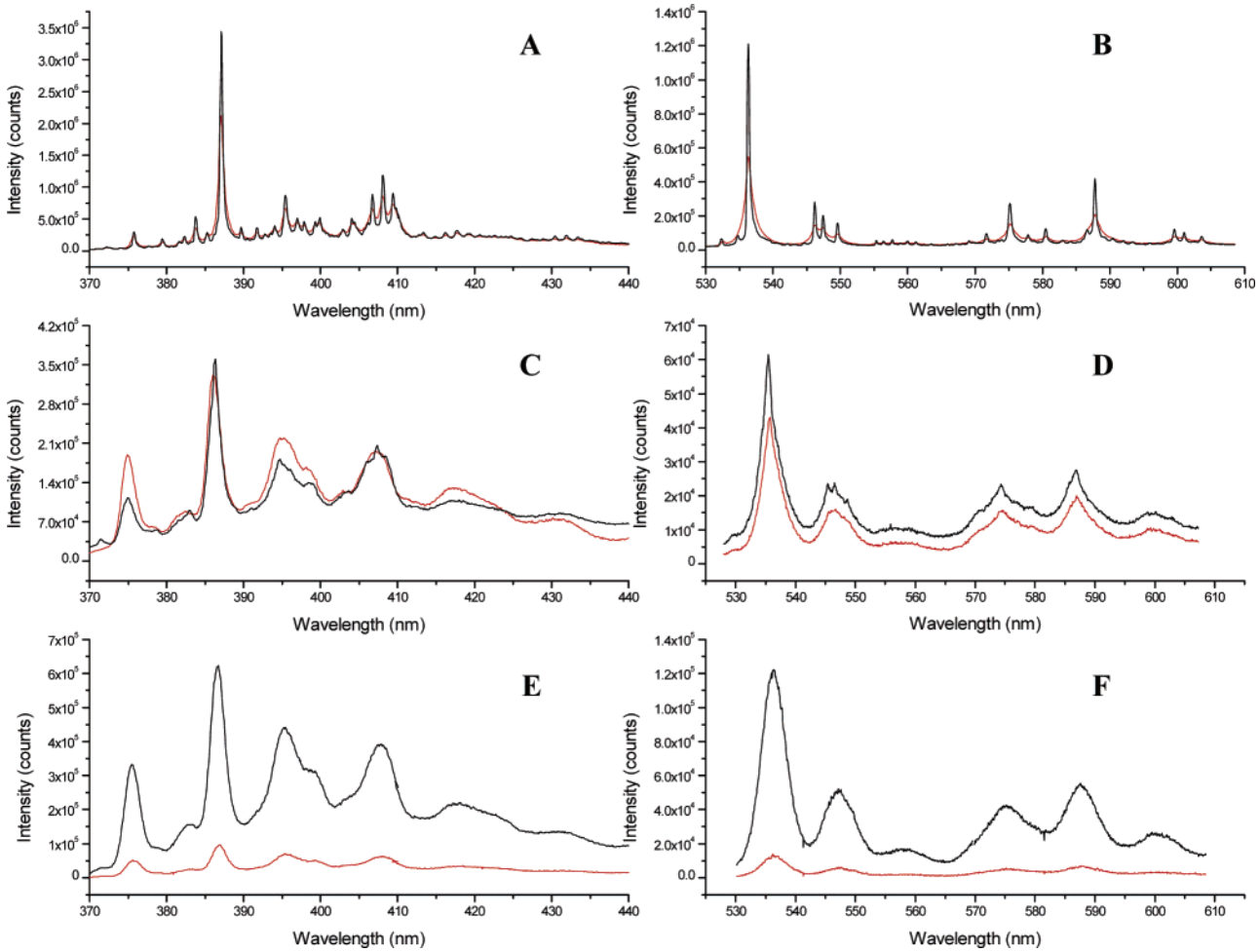

Figure 4. Fluorescence and phosphorescence spectra of 0.5 $\mu g \cdot mL^{-1}$ benzo[*e*]pyerene at 77 (black) and 4.2 K (red) in three matrixes. (A) fluorescence and (B) phosphorescence in *n*-octane, (C) fluorescence and (D) phosphorescence in methanol, and (E) fluorescence and (F) phosphorescence on extraction membranes. Excitation wavelength was 387.1 nm. Fluorescence spectra were collected using delay and gate times of 20 and 200 ns, respectively. Phosphorescence spectra were collected using a delay of 10 μs and a gate of 40 ms. All spectra correspond to the accumulation of 100 laser shots. Slit width of spectrograph, 40 μm.

Table 3. 4.2 K Fluorescence and Phosphorescence Intensities[a] of PAHs in Shpol'skii, Methanol, and Extraction Membranes

PAH[b]	λ (nm)	*n*-octane	methanol	extraction membrane
chrysene	359.6[c]	499.46 ± 20.25 (4.05)	4.99 ± 0.17 (3.41)	42.84 ± 3.28 (7.66)
	499.1[d]	105.27 ± 4.53 (4.30)	13.62 ± 0.74 (5.49)	1.32 ± 0.76 (5.82)
benzo[*e*]pyerene	387.1[c]	85.76 ± 3.63 (4.23)	5.56 ± 0.25 (4.5)	706.84 ± 38.82 (5.49)
	536.8[d]	20.18 ± 0.62 (3.10)	6.29 ± 0.35 (5.56)	217.42 ± 11.63 (5.35)
benzo[*ghi*]perylene	406.5[c]	3,723.70 ± 153.54 (4.12)	7.31 ± 0.34 (4.72)	266.97 ± 17.93 (6.72)
	614.6[d]	284.40 ± 9.69 (3.41)	*f*	*f*

[a] Intensities in $\times 10^3$ counts. Values in parentheses represent the relative standard deviations (%) of six measurements taken from six separate sample aliquots. [b] All concentrations were 0.2 $\mu g \cdot mL^{-1}$. Excitation wavelength was 321.4 nm for chrysene, 320.4 nm for benzo[*e*]pyrene, and 386.8 nm for benzo[*ghi*]perylene. [c] Maximum fluorescence wavelength. [d] Maximum phosphorescence wavelength. [f] No phosphorescence was observed for this PAH−matrix combination.

Table 4. 4.2 K Fluorescence and Phosphorescence Lifetimes[a] of PAHs in Shpol'skii, Methanol, and Extraction Membranes

PAH[b]	λ (nm)	*n*-octane	methanol	extraction membrane
benzo[*ghi*]perylene	387.1[c]	199.9 ± 1.7 ns (0.8)	145.1 ± 2.8 ns (1.9)	135.4 ± 1.0 ns (0.7)
	536.8[d]	292 ± 4 ms (1.5)	*e*	*e*
chrysene	359.6[c]	63.4 ± 1.0 ns (1.6)	59.1 ± 1.9 ns (3.2)	26.9 ± 0.8 ns (2.9)
	499.1[d]	2078 ± 32 ms (1.5)	2643 ± 51 ms (1.9)	1,980 ± 56.4 ms (2.8)
benzo[*e*]pyerene	406.5[c]	57.9 ± 1.3 ns (2.2)	66.9 ± 1.9 ns (2.8)	62.9 ± 1.7 ns (2.7)
	614.6[d]	1,780 ± 30 ms (1.7)	1,889 ± 2.5 ms (0.1)	1,824 ± 31.2 ms (1.7)

[a] Values in parentheses represent the relative standard deviations (%) of six measurements taken from six separate sample aliquots. [b] All concentrations were 0.2 $\mu g \cdot mL^{-1}$. Excitation wavelength was 321.4 nm for chrysene, 320.4 nm for benzo[*e*]pyrene, and 386.8 nm for benzo[*ghi*]perylene. [c] Maximum fluorescence wavelength. [d] Maximum phosphorescence wavelength. [e] No phosphorescence was observed for this PAH−matrix combination.

reported with other PAHs/alkane Shpol'skii systems,[22] the three fluorescence sites show statistically different lifetimes ($\alpha = 0.05$, $N_1 = N_2 = N_3 = 6$).[30] The same is true for the phosphorescence lifetimes. The comparison of the relative standard deviations shows excellent precision of measurements within the entire luminescence time domain (ns−s).

Luminescence Measurements in Highly Scattering Media. Conventional low-temperature spectroscopy has been restricted to optically transparent media. This restriction has limited its application to solvents that freeze into a glass. The FOP removes this limitation and allows one to measure luminescence from highly scattering media such as snowlike matrixes and solid samples. Figure 4 shows the fluorescence and phosphorescence spectra of benzo[*e*]pyrene recorded from *n*-octane (optically transparent) and methanol (snow) and extracted on an octadecyl membrane (solid sample). Emission spectra in *n*-octane exhibit considerable narrowing upon cooling to 77 and 4.2 K. Both spectra are consistent with single-site emission of benzo[*e*]pyrene in this Shpol'skii matrix. When in methanol and on the extraction membrane, benzo[*e*]pyrene shows broader spectra. The reduced narrowing with respect to *n*-octane is due to the inhomogeneous nature of methanol and the membrane. In these two media, homogeneous broadening still exists and the spectra get narrower only because the Boltzman distribution is narrowed. Interesting to note is the intensity enhancement observed on extraction membranes upon cooling from 77 to 4.2 K. Because temperature enhancements were not observed in *n*-octane and methanol, the nonradiative processes for the deactivation of the first singlet and triplet excited states might be closely related to the sample temperature (77 K and below) only on extraction membranes.

Table 3 lists the 4.2 K luminescence intensities (peak heights) from three PAHs in the three sample matrixes. Although the signal intensities for all three PAHs were larger in *n*-octane than in methanol, the relative standard deviations are comparable. These demonstrate the ability of the FOP to perform low-temperature measurements in "snowy" matrixes with precision similar to that in Shpol'skii matrixes. A similar statement can be made for lifetime measurements (see Table 4). It is interesting to note the better precision of lifetime measurements. This is mostly due to the nature of lifetime measurements, where the ratio between signal intensities cancels out variations of instrumental response.

When adsorbed onto the octadecyl membrane, all three PAHs exhibit large intensity variations. This is not surprising because the background emission of extraction membranes varies considerably from disk to disk and measuring wavelengths.[32,33] The phosphorescence of benzo[*ghi*]perylene in methanol and on extraction membranes was extremely weak. In fact, at concentrations of 50 $\mu g \cdot mL^{-1}$, its phosphorescence intensity did not exceed 2 times the noise. The collection of phosphorescence spectra and lifetimes for benzo[*ghi*]perylene in methanol and on membranes was, therefore, not possible at those experimental conditions.

Excitation−Emission Spectra of PAHs in Different Types of Matrixes. Panels A and B in Figure 5 display the 4.2 K fluorescence and phosphorescence EEM of chrysene in *n*-octane, respectively. The EEMs show identical features, which are shifted in both emission and excitation from one another. This effect is often an indication that multiple sites are present. Given the

(31) Nakhimovsky, I. A.; Lamotte, M.; Joussot-Dubien, J. *Handbook of Low-Temperature Electronic Spectra of Polycyclic Aromatic Hydrocarbons*; Elsevier: Amsterdam, 1989.
(32) Whitcomb, J. L.; Bystol, A. J.; Campiglia, A. D. *Anal. Chim. Acta* **2002**, *464*, 261−272.
(33) Arruda A. F.; Campiglia, A. D. *Environ. Sci. Technol.* **2000**, *34*, 4982−4988.

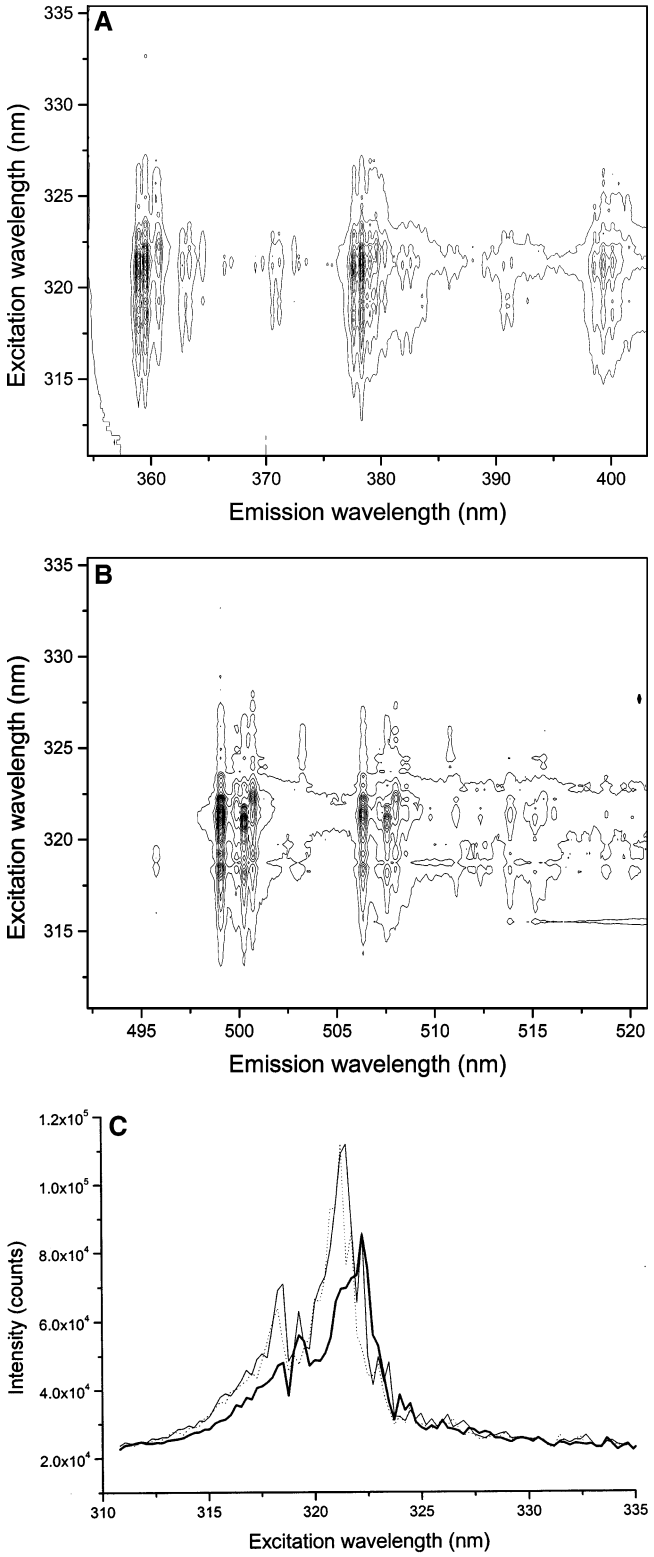

Figure 5. 4.2 K fluorescence (A) and phosphorescence (B) EEM for 0.2 μg·mL^{-1} chrysene in *n*-octane. The fluorescence EEM was recorded using a 20-ns delay and a 200-ns gate times. The phosphorescence EEM was collected using 10-μs delay and 40-ms gate times. Excitation wavelength step was 0.1 nm. (C) Fluorescence excitation spectra stripped from the EEM at 359.2 (—), 359.6 (- - -), and 360.6 nm (—).

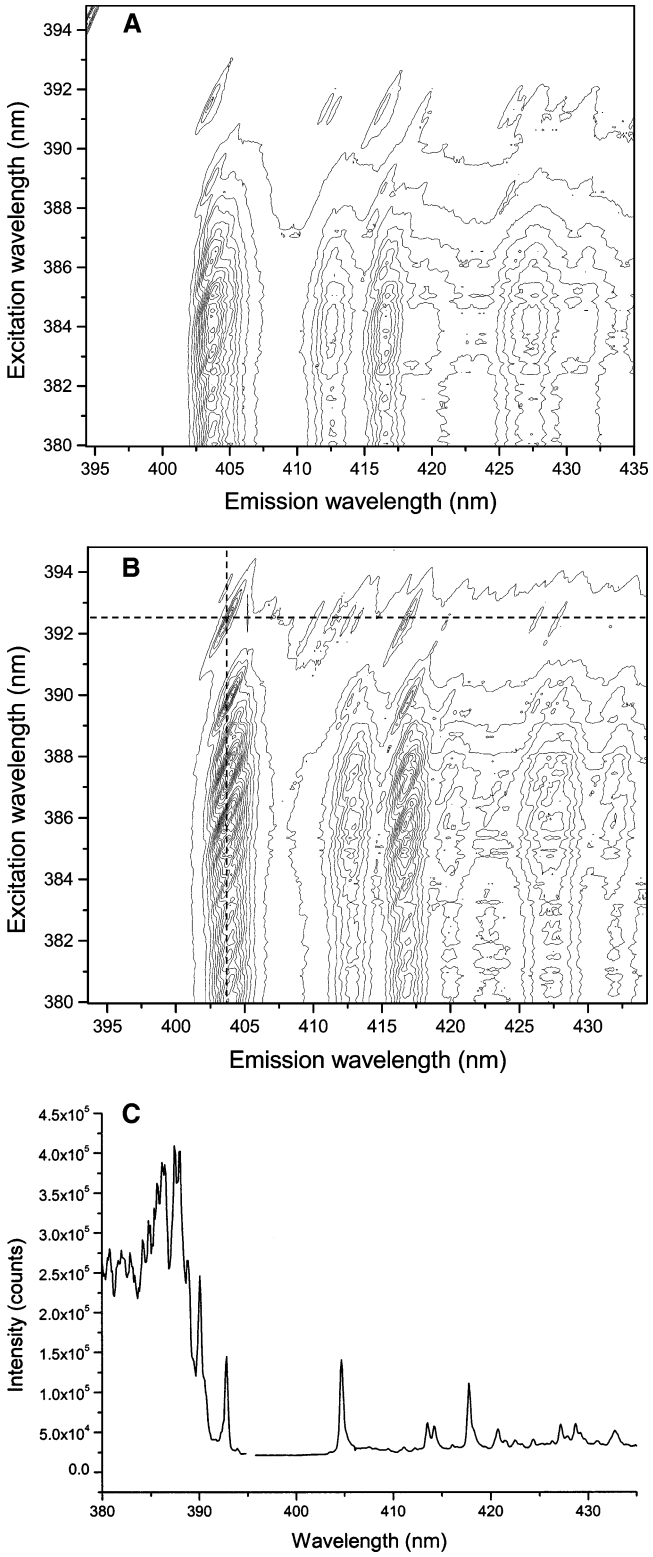

Figure 6. 4.2 K fluorescence EEM for 0.2 μg·mL^{-1} benzo[*ghi*]-perylene in methanol (A) and on the extraction membrane (B). Both EEM were recorded using a 20-ns delay and a 2000-ns gate times. Excitation wavelength step was 0.1 nm. (C) Excitation and emission spectra corresponding to data from dotted lines in (B).

multiplet structure of emission—which was confirmed via lifetime measurements—this situation is most likely the case. The vertical features correspond to the emission at one wavelength as a function of excitation wavelength. Plotting these data as a two-dimensional graph produces the excitation spectrum. Figure 5C shows the excitation spectra of the three site phosphorescence

wavelengths of chrysene in *n*-octane. The spectra present very similar excitation profiles shifted within a few nanometers of one another.

When inhomogeneous matrixes are employed, EEMs can provide valuable data relating the line narrowing behavior with the excitation profile. Panels A and B in Figure 6 show the 4.2 K fluorescence EEMs collected from benzo[*ghi*]perylene in methanol and on the extraction membrane, respectively. In both EEMs, diagonal features appear at excitation wavelengths above 388 nm. These diagonal features correspond to fluorescence line narrowing of benzo[*ghi*]perylene. As the excitation wavelength is tuned through this region, the narrowed emission spectra shift the emission wavelength at the same rate as the excitation wavelength. Figure 6C shows the two-dimensional excitation and line-narrowed fluorescence spectra of benzo[*ghi*]perylene on the extraction membrane, corresponding to the dotted lines in Figure 6B. An excitation wavelength of 392.5 nm was used for the emission spectrum, and an emission wavelength of 403.2 nm was used for the excitation spectrum.

CONCLUSIONS

An instrument with the capability to collect multidimensional fluorescence and phosphorescence data formats has been presented. The integration of a pulsed tunable dye laser, a mechanical shutter, a spectrograph, an ICCD, and custom data acquisition software has made possible the collection of WTMs, EEMs, and TREEMs within the entire time domain of luminescence (ns−s). This capability makes our instrument the appropriate tool for those applications seeking the full dimensionality of luminescence spectroscopy, including approaches based on room-temperature luminescence techniques. It is now possible to collect numerous qualitatitive parameters with a single instrument. The extension of the fiber-optic probe beyond Shpol'skii matrixes has been demonstrated with accurate and precise measurements in optically scattering media at 77 and 4.2 K. Because sample freezing with the fiber-optic probe is rapid and straightforward, the benefits of lowering the temperature are now available without the traditional constrains associated to cumbersome experimental procedures.

ACKNOWLEDGMENT

This research was supported by the National Science Foundation (CHE-0138093).

Received for review July 26, 2005. Accepted November 10, 2005.

AC051332V